

# Characteristics of AlGaIn/GaN/AlGaIn double heterojunction HEMTs with an improved breakdown voltage\*

Ma Juncai(马俊彩)<sup>†</sup>, Zhang Jincheng(张进成), Xue Junshuai(薛军帅), Lin Zhiyu(林志宇), Liu Ziyang(刘子扬), Xue Xiaoyong(薛晓咏), Ma Xiaohua(马晓华), and Hao Yue(郝跃)

Key Laboratory of Wide Band Gap Semiconductor Materials and Devices, School of Microelectronics, Xidian University, Xi'an 710071, China

**Abstract:** We studied the performance of AlGaIn/GaN double heterojunction high electron mobility transistors (DH-HEMTs) with an AlGaIn buffer layer, which leads to a higher potential barrier at the backside of the two-dimensional electron gas channel and better carrier confinement. This, remarkably, reduces the drain leakage current and improves the device breakdown voltage. The breakdown voltage of AlGaIn/GaN double heterojunction HEMTs ( $\sim 100$  V) was significantly improved compared to that of conventional AlGaIn/GaN HEMTs ( $\sim 50$  V) for the device with gate dimensions of  $0.5 \times 100 \mu\text{m}$  and a gate-drain distance of  $1 \mu\text{m}$ . The DH-HEMTs also demonstrated a maximum output power of  $7.78$  W/mm, a maximum power-added efficiency of  $62.3\%$  and a linear gain of  $23$  dB at the drain supply voltage of  $35$  V at  $4$  GHz.

**Key words:** AlGaIn/GaN/AlGaIn double heterojunctions; breakdown voltage; carrier confinement

**DOI:** 10.1088/1674-4926/33/1/014002

**EEACC:** 2570

## 1. Introduction

In recent decades, due to unique characteristics such as a wide band-gap, superior carrier saturation velocity, a large breakdown field strength and strong spontaneous and piezoelectric polarization, GaN-based high-electron mobility transistors (HEMTs) have attracted considerable attention and shown excellent performance in high-power and high-frequency electronics applications<sup>[1–3]</sup>. Although remarkable progress has been achieved for AlGaIn/GaN single heterojunction (SH) HEMTs due to improved material quality and process techniques, there still remain some obstacles. In the conventional AlGaIn/GaN HEMT structure, the two-dimensional electron gas (2DEG) induced by spontaneous and piezoelectric polarization is confined in an approximately triangular potential well formed at the interface between the AlGaIn barrier and GaN buffer. However, due to the lower potential barrier height of the GaN buffer layer, also known as the insufficient confinement of the 2DEG in the channel, it is easy for the 2DEG to overflow from the potential well into the GaN buffer layer, thus causing a buffer layer punchthrough effect and deterioration of the transport characteristics. In many cases, such as at high temperatures, high 2DEG density or a more negative gate voltage, part of the 2DEG can spill over from the potential well and become three-dimensional electrons, which lead to an apparent decrease of average electron mobility, because the mobility of three-dimensional electrons ( $200\text{--}500 \text{ cm}^2/(\text{V}\cdot\text{s})$ ) is much less than that of two-dimensional electrons ( $1000\text{--}2000 \text{ cm}^2/(\text{V}\cdot\text{s})$ )<sup>[4]</sup>. In order to overcome the limitations of the conventional SH-HEMTs, several methods were proposed, such as using a Mg- or C-doped GaN buffer

layer<sup>[5]</sup>, inserting an InGaIn layer into the GaN buffer layer (AlGaIn/GaN/InGaIn/GaN heterojunctions)<sup>[6]</sup> or using an AlGaIn buffer layer (AlGaIn/GaN/AlGaIn double heterojunctions)<sup>[7]</sup>. In double heterojunctions, the channel is separated from the buffer layer due to the second heterojunction at the bottom side of the channel. The additional barrier leads to better carrier confinement and buffer isolation, as well as improved device performance, such as a lower buffer leakage current and a higher power gain cutoff frequency.

In this paper, AlGaIn/GaN double heterojunction (DH) HEMTs with an AlGaIn buffer layer with a low Al composition of about  $7\%$  were fabricated. We focus on the growth and characteristics of AlGaIn buffer DH-HEMTs, which demonstrate an improved breakdown voltage and decreased off-state drain leakage current compared with conventional AlGaIn/GaN HEMTs. A power added efficiency of  $62.3\%$  and a maximum output power of  $7.78$  W/mm were obtained for the DH-HEMT device at a drain supply voltage of  $35$  V at  $4$  GHz.

## 2. Experiments

All the GaN heterojunctions were grown by low-pressure metal organic chemical vapor deposition (MOCVD) on 2-inch semi-insulating 4H-SiC substrates. Trimethylaluminum (TMAI), triethylgallium (TEGa) and ammonia ( $\text{NH}_3$ ) were used as the sources of Al, Ga and N, respectively. Hydrogen was used as a carrier gas. After annealing the substrate in a  $\text{H}_2$  environment for  $10$  min at  $1050$  °C, a  $100$  nm high temperature AlN nucleation layer was grown at  $1050$  °C, followed by a  $1.5 \mu\text{m}$   $\text{Al}_{0.07}\text{Ga}_{0.93}\text{N}$  buffer layer. Then a  $10$  nm nominally undoped GaN layer was deposited as a 2DEG channel followed

\* Project supported by the National Science and Technology Major Project of the Ministry of Science and Technology of China (No. 2008ZX01002-002) and the Major Program and the Key Program of the National Natural Science Foundation of China (Nos. 60890191, 60736033).

<sup>†</sup> Corresponding author. Email: majuncai1609@163.com

Received 18 July 2011, revised manuscript received 8 August 2011

© 2012 Chinese Institute of Electronics

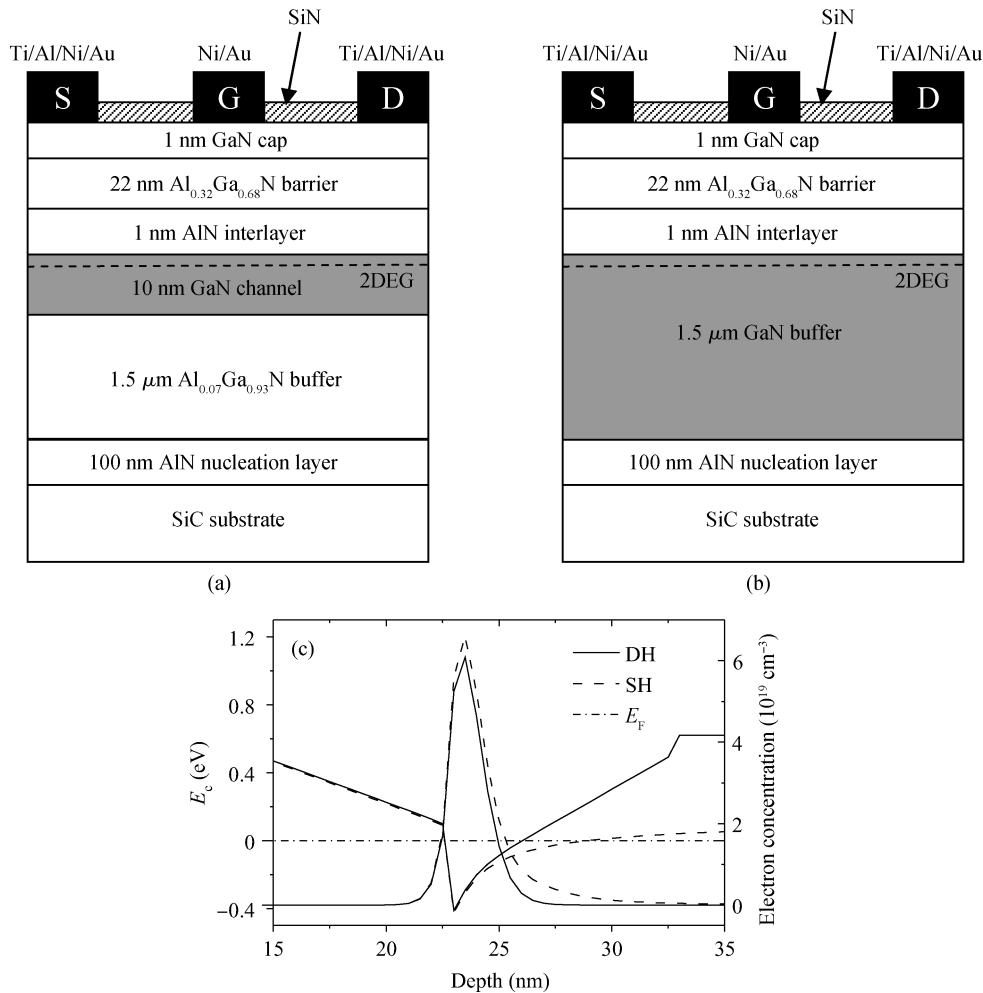


Fig. 1. Schematic cross sections of (a) AlGaN/GaN/AlGaN DH and (b) AlGaN/GaN SH and (c) the calculated conduction band diagrams and electron distributions of the DH and SH.

by a 1 nm AlN interlayer. Finally, a 22 nm top Al<sub>0.32</sub>Ga<sub>0.68</sub>N barrier layer and a 1 nm GaN cap layer were deposited. For comparison, a conventional single heterojunction was grown using a 1.5 μm GaN buffer layer instead of the AlGaN buffer layer, and the other layers were grown in the same conditions as the DH. The schematic cross sections of the two structures are shown in Figs. 1(a) and 1(b). The conduction band diagrams and electron distributions of DH and SH achieved by self-consistently solving a one-dimensional Poisson–Schrödinger equation are also shown in Fig. 1(c), which indicates that the 2DEG confinement is improved in DH-HEMT due to the increased back-barrier height of the AlGaN buffer.

The device fabrication of the two structures is identical and starts with mesa isolation using inductively coupled plasma (ICP) dry etching. Then, Ti/Al/Ni/Au metals were deposited as source and drain ohmic contacts by electron beam evaporation, followed by rapid thermal annealing at 870 °C for 40 s in ambient N<sub>2</sub>. The Ni/Au Schottky gate was defined by optical stepper lithography with a gate length of 0.5 μm and gate width of 100 μm. Finally, a SiN passivation layer was deposited by PECVD. Both the gate–source distance and gate–drain distance for the SH and DH HEMTs were 1 μm.

The crystal quality and reciprocal lattice mapping of the two heterostructures were characterized by high-resolution

X-ray diffraction (HRXRD) (Bruker D8 Discover HRXRD diffractometer). The Hall Effect measurement was carried out using a van der Pauw technique at room temperature to characterize the electrical properties. Additionally, Raman spectroscopy was used to analyze the Al composition in the AlGaN buffer layer using a 514 nm argon ion laser with Z(XX)-Z scattering geometry at room temperature (JY LabRam HR800). The device direct current (DC) performances were measured by Agilent 1500A semiconductor parameter analyzers. Large-signal load-pull measurements were conducted on the two kinds of devices at 4 GHz using a Maury load-pull system.

### 3. Results and discussion

Since the Al composition of the AlGaN buffer layer is a decisive parameter for the back-barrier height, the Raman characterization was performed and the spectra were presented in Fig. 2. The A<sub>1</sub>(LO) mode and E<sub>2</sub>(high) mode of the AlGaN buffer layer is located at 750 and 571 cm<sup>-1</sup>, respectively. Because the A<sub>1</sub>(LO) mode is more sensitive to Al composition *x*, a quadratic equation is proposed to conveniently estimate *x* as follows: A<sub>1</sub>(LO)<sub>Al<sub>x</sub>Ga<sub>1-x</sub>N</sub> = 734 + 153*x* + 75*x*(1 - *x*)<sup>[8]</sup>. Therefore, according to A<sub>1</sub>(LO)<sub>Al<sub>x</sub>Ga<sub>1-x</sub>N</sub> = 750 cm<sup>-1</sup>, the Al composition in the AlGaN buffer can be calculated to be ap-

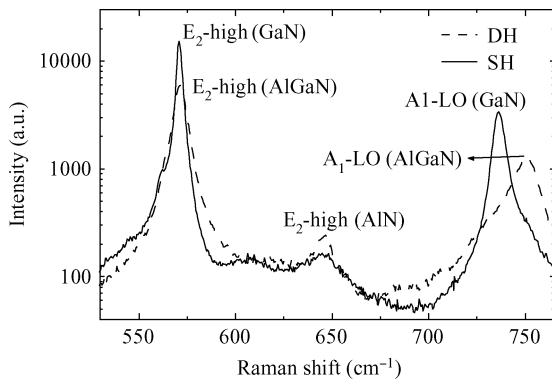


Fig. 2. Raman spectra of DH and SH grown on SiC substrates.

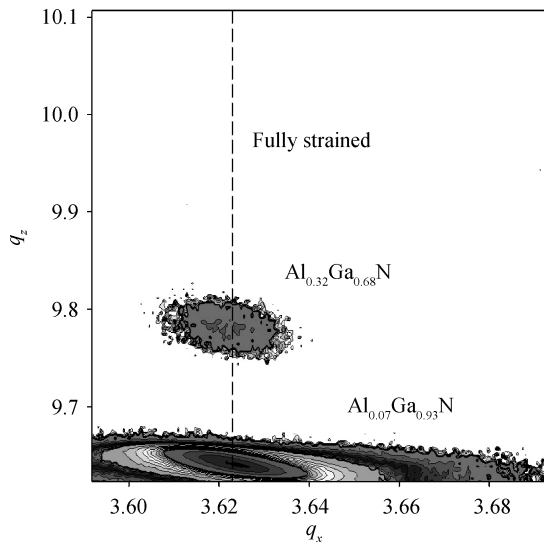


Fig. 3. X-ray reciprocal space map around the asymmetrical (10 $\bar{1}$ 5) diffraction of the DH-HEMT structure with an Al<sub>0.07</sub>Ga<sub>0.93</sub>N buffer layer.

proximately 7%, which is in good agreement with our experiment design.

A Hall measurement was performed with a Hall-bridge pattern fabricated on both the SH-HEMT and DH-HEMT wafers. A 2DEG mobility of 1713 cm<sup>2</sup>/(V·s) and a sheet carrier density of 8.48 × 10<sup>12</sup> cm<sup>-2</sup> were obtained at room temperature on the AlGaN/GaN/AlGaN DH-HEMT sample. Our conventional AlGaN/GaN SH-HEMT structure exhibits a 2DEG mobility of 1605 cm<sup>2</sup>/(V·s) and a sheet carrier density of 1.07 × 10<sup>13</sup> cm<sup>-2</sup>. The sheet resistances of DH and SH structures are 372 Ω/□ and 309 Ω/□, respectively. The lower carrier density and higher 2DEG mobility in DH-HEMT are mainly attributed to the raised conduction band of the AlGaN back-barrier layer, which enables an enhanced 2DEG confinement and thus a deeper and narrower channel, which is consistent with the calculated conduction band diagram and electron distribution as shown in Fig. 1(c).

To further study the strain state in the DH-HEMT epitaxial structure, an XRD reciprocal space mapping (RSM) measurement was carried out around the asymmetric (10 $\bar{1}$ 5) plane. Compared with the diffraction patterns in one-dimensional angular distribution, two-dimensional RSM is a direct and effective

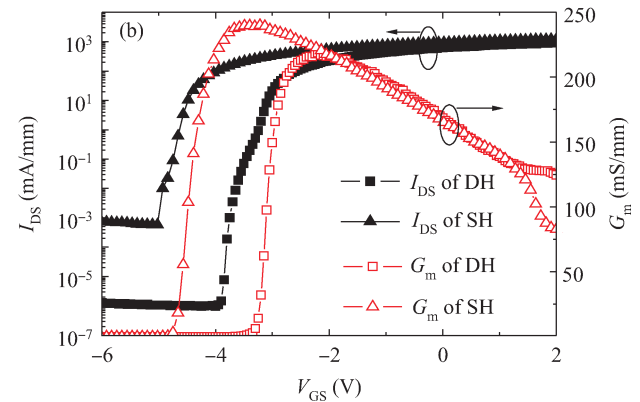
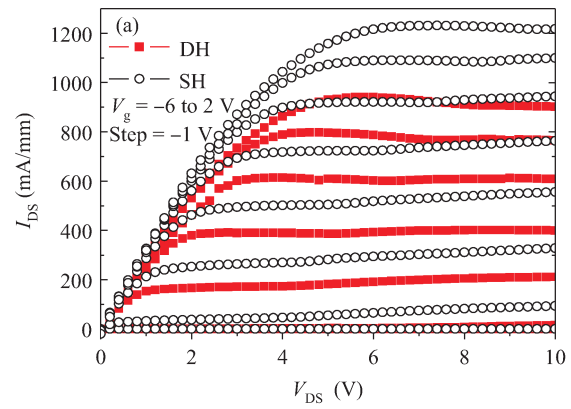


Fig. 4. DC characteristics of AlGaN/GaN DH-HEMTs (square) and SH-HEMTs (triangle). (a)  $I_{DS}$ - $V_{DS}$  curves, where  $V_{GS}$  starts from +2 V at the top with a step of -1 V. (b)  $I_{DS}$ - $V_{GS}$  and  $G_m$ - $V_{GS}$  curves.

tool to determine the strain state in the heterojunctions and gives better precision. Figure 3 displays the reciprocal space mapping for (10 $\bar{1}$ 5) reflection of the DH-HEMT epitaxial structure. The dashed line indicates the position of the fully strained top AlGaN barrier layer. As shown in the figure, the two domains corresponding to the Al<sub>0.07</sub>Ga<sub>0.93</sub>N buffer and the Al<sub>0.32</sub>Ga<sub>0.68</sub>N barrier are clearly separated. The domain corresponding to the top Al<sub>0.32</sub>Ga<sub>0.68</sub>N barrier is aligned to the domain of the Al<sub>0.07</sub>Ga<sub>0.93</sub>N buffer layer along  $q_x$ , which demonstrates that the top Al<sub>0.32</sub>Ga<sub>0.68</sub>N barrier is fully strained to the 1.3 μm Al<sub>0.07</sub>Ga<sub>0.93</sub>N buffer layer in the DH-HEMT structure.

DC measurements of the devices were carried out to study the device performances fabricated on the above different samples. The gate dimensions of the devices are 0.5 × 100 μm<sup>2</sup>. The typical current-voltage and transfer characteristic of the DH-HEMTs are plotted and compared with those of the conventional AlGaN/GaN SH-HEMTs in Figs. 4(a) and 4(b). The maximum drain current density of the DH-HEMT device is about 940 mA/mm at  $V_{DS} = 10$  V and  $V_{GS} = 2$  V, which is lower than the conventional one (~1230 mA/mm). The peak transconductance of the DH-HEMT device, as shown in Fig. 4(b), is about 220 mS/mm, which is a little lower than the value of our conventional SH-HEMT device (~240 mS/mm). The decreased maximum drain current and peak transconductance of the DH-HEMT result from the lower 2DEG density in the channel. The threshold voltage of the DH-HEMT is -3.0 V, which shifted positively compared to that of the conventional

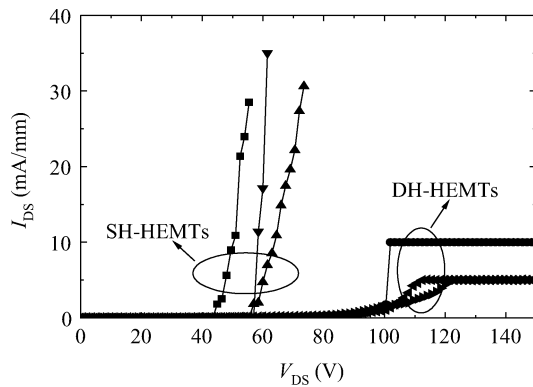


Fig. 5. Off-state breakdown characteristics of conventional AlGaIn/GaN HEMTs and AlGaIn/GaN/AlGaIn DH-HEMTs at a gate voltage of  $-8$  V.

SH-HEMT ( $-4.4$  V). This difference is caused by the different carrier concentration in the 2DEG channel between the DH-HEMT sample and the conventional SH-HEMT sample. The SH-HEMT structure has a larger 2DEG density and needs a more negative voltage to deplete the channel. In addition, from the measurement results it can be seen that one of the advantages of the DH-HEMT over the conventional SH-HEMT is the lower buffer leakage current, which is  $1.3 \times 10^{-6}$  mA/mm at  $V_{DS} = 10$  V and  $V_{GS} = -6$  V for the DH-HEMT. This is significantly lower than that in our conventional SH-HEMT ( $7.5 \times 10^{-4}$  mA/mm). The reduced off-state drain leakage current in the DH-HEMTs strongly indicates that the increase of the effective potential barrier provided by the AlGaIn buffer layer below the 2DEG channel can effectively prevent the electrons spilling over from the channel to the buffer under the high drain voltage and improve buffer isolation.

The off-state  $I_{DS}-V_{DS}$  characteristics of conventional AlGaIn/GaN HEMTs and AlGaIn/GaN/AlGaIn DH-HEMTs with a wide drain bias region at the gate voltage of  $-8$  V are shown in Fig. 5. The conventional HEMTs and DH-HEMTs demonstrate the off-state breakdown voltages of  $\sim 50$  and  $\sim 100$  V, respectively, which indicate that the breakdown characteristic of the DH-HEMT device with an AlGaIn buffer layer has been significantly improved from that of the conventional AlGaIn/GaN HEMT. As mentioned above, the electrons spilling over from the channel to the buffer layer at a high drain supply voltage can form the buffer leakage current. In many cases, breakdown in GaN-based HEMTs is initiated by the electron current underneath the depletion region of the gate through the insulating buffer layer and is known as the buffer-layer punchthrough effect<sup>[9]</sup>. The punchthrough of the electrons into the buffer layer causes a rapid increase of the drain leakage current and the device breakdown occurs when the drain leakage current exceeds a certain value, such as 10 mA/mm<sup>[10]</sup>. It is believed that enhancement of the off-state breakdown voltage of the DH-HEMT device is attributed to a better carrier confinement in the DH-HEMT. The increased back-barrier height of the AlGaIn buffer layer suppresses the spillover of the 2DEG into the buffer layer and postpones the punchthrough of the buffer layer, thus reducing the subthreshold drain leakage current and increasing the breakdown voltage remarkably.

Large-signal load-pull measurements were also conducted

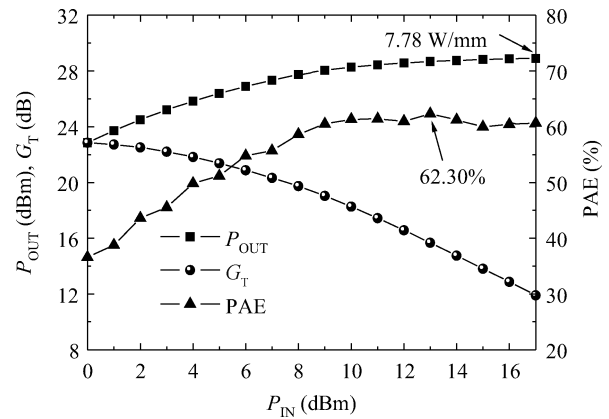


Fig. 6. Power performance of  $0.5 \times 100 \mu\text{m}$  AlGaIn/GaN/AlGaIn DH-HEMT devices measured at 4 GHz, with a drain supply voltage of 35 V.

on AlGaIn/GaN/AlGaIn DH-HEMT devices at 4 GHz using a Maury load-pull system. For a device with gate dimensions of  $0.5 \times 100 \mu\text{m}$ , a maximum power added efficiency of 62.3%, associated with a power density of 7.37 W/mm was obtained at a drain supply voltage of 35 V, as shown in Fig. 6. The device also demonstrated a linear gain of 23 dB and a maximum output power density of 7.78 W/mm.

## 4. Conclusions

AlGaIn/GaN/AlGaIn DH-HEMTs with an  $\text{Al}_{0.07}\text{Ga}_{0.93}\text{N}$  buffer layer grown by MOCVD on 4H-SiC substrates was investigated. The maximum drain current and maximum transconductance were about 940 mA/mm and 220 mS/mm, respectively. Compared with conventional SH-HEMTs using a GaN buffer layer, AlGaIn/GaN DH-HEMTs with an  $\text{Al}_{0.07}\text{Ga}_{0.93}\text{N}$  buffer layer demonstrated a remarkable enhancement of breakdown voltage and decrease of the off-state drain leakage current due to the effective improvement of carrier confinement as a result of the improved back-barrier height. The DH-HEMT device also demonstrated a maximum output power of 7.78 W/mm and a maximum power-added efficiency of 62.3% at the drain supply voltage of 35 V at 4 GHz. The results imply that an AlGaIn/GaN DH-HEMT is a promising structure for higher-voltage and higher-power device applications. Meanwhile, the properties of AlGaIn/GaN/AlGaIn DH-HEMTs are expected to be improved by reducing the crystal defects in the AlGaIn buffer layer by optimizing the growth conditions.

## References

- [1] Yu H B, Lisesivdin S B, Bolukbas B, et al. Improvement of breakdown characteristics in AlGaIn/GaN/ $\text{Al}_x\text{Ga}_{1-x}\text{N}$  HEMT based on a grading  $\text{Al}_x\text{Ga}_{1-x}\text{N}$  buffer layer. *Phys Status Solidi A*, 2010, 11: 2593
- [2] Quan S, Hao Y, Ma X H, et al. AlGaIn/GaN double-channel HEMT. *Journal of Semiconductors*, 2010, 31: 044003
- [3] Chen C Q, Zhang J P, Adivarahan V, et al. AlGaIn/GaN/AlGaIn double heterostructure for high-power III-N field-effect transistors. *Appl Phys Lett*, 2003, 82: 4593

- [4] Nakamura S. GaN growth using GaN buffer layer. *Jpn J Appl Phys*, 1991, 30: L1705
- [5] Chen Z, Pei Y, Chu R, et al. Growth and characterization of AlGa<sub>N</sub>/Ga<sub>N</sub>/AlGa<sub>N</sub> field effect transistors. *Phys Status Solidi C*, 2010, 7: 2404
- [6] Liu J, Zhou Y G, Zhu J, et al. AlGa<sub>N</sub>/Ga<sub>N</sub>/InGa<sub>N</sub>/Ga<sub>N</sub> DH-HEMTs with an InGa<sub>N</sub> notch for enhanced carrier confinement. *IEEE Electron Device Lett*, 2006, 27: 10
- [7] Bahat-Treidel E, Hilt O, Brunner F, et al. AlGa<sub>N</sub>/Ga<sub>N</sub>/AlGa<sub>N</sub> DH-HEMTs breakdown voltage enhancement using multiple grating field plates (MGFPs). *IEEE Trans Electron Devices*, 2010, 57: 1208
- [8] Harima H. Properties of GaN and related compounds studied by means of Raman scattering. *J Phys: Condensed Matter*, 2002, 14: R967
- [9] Uren M J, Nash K J, Balmer R S, et al. Punch-through in short-channel AlGa<sub>N</sub>/Ga<sub>N</sub> HFETs. *IEEE Trans Electron Devices*, 2006, 53: 395
- [10] Bahat-Treidel E, Hilt O, Brunner F, et al. Punchthrough-voltage enhancement of AlGa<sub>N</sub>/Ga<sub>N</sub> HEMTs using AlGa<sub>N</sub> double-heterojunction confinement. *IEEE Trans Electron Devices*, 2008, 55: 12